Article

Synthesis of Ethanol from Syngas over Rh/MCM-41 Catalyst: Effect of Water on Product Selectivity

Luis Lopez [1,2,*]**, Jorge Velasco** [1,2]**, Vicente Montes** [3]**, Alberto Marinas** [3]**, Saul Cabrera** [2]**, Magali Boutonnet** [1] **and Sven Järås** [1]

[1] KTH Royal Institute of Technology, Chemical Technology, Teknikringen 42,
SE-100 44 Stockholm, Sweden; E-Mails: javc@kth.se (J.V.); magalib@kth.se (M.B.);
sjaras@kth.se (S.J.)

[2] UMSA Universidad Mayor de San Andrés, Instituto del Gas Natural, Campus Universitario, La Paz,
Bolivia; E-Mail: saulcabreram@hotmail.com

[3] Organic Chemistry Department, University of Córdoba, ceiA3, Marie Curie Building,
E-14014 Córdoba, Spain; E-Mails: q22mojiv@uco.es (V.M.); qo2maara@uco.es (A.M.)

* Author to whom correspondence should be addressed; E-Mail: lgln@kth.se;
Tel.: +46-8-790-8245.

Academic Editor: Michalis Konsolakis

Abstract: The thermochemical processing of biomass is an alternative route for the manufacture of fuel-grade ethanol, in which the catalytic conversion of syngas to ethanol is a key step. The search for novel catalyst formulations, active sites and types of support is of current interest. In this work, the catalytic performance of an Rh/MCM-41 catalyst has been evaluated and compared with a typical Rh/SiO$_2$ catalyst. They have been compared at identical reaction conditions (280 °C and 20 bar), at low syngas conversion (2.8%) and at same metal dispersion (H/Rh = 22%). Under these conditions, the catalysts showed different product selectivities. The differences have been attributed to the concentration of water vapor in the pores of Rh/MCM-41. The concentration of water vapor could promote the water-gas-shift-reaction generating some extra carbon dioxide and hydrogen, which in turn can induce side reactions and change the product selectivity. The extra hydrogen generated could facilitate the hydrogenation of a C$_2$-oxygenated intermediate to ethanol, thus resulting in a higher ethanol selectivity over the Rh/MCM-41 catalyst as compared to the typical Rh/SiO$_2$ catalyst; 24% and 8%, respectively. The catalysts have been characterized, before and after reaction, by N$_2$-physisorption, X-ray photoelectron

spectroscopy, X-ray diffraction, H_2-chemisorption, transmission electron microscopy and temperature programmed reduction.

1. Introduction

At present, fuel-grade ethanol is utilized as a renewable component in gasoline or as a pure fuel in flex-fuel vehicles [1,2]. In 2013, about 70 million tons of fuel-grade ethanol were produced worldwide [3]. Most of the production technologies use food-related raw materials, such as corn in the USA or sugar cane in Brazil. Non-food related resources such as forest and agricultural biomass (known as cellulosic biomass) are being considered as alternative raw materials. Indeed, several public and private institutions have started R&D programs in order to produce fuel-grade ethanol from cellulosic biomass, at competitive cost [4].

In principle, any kind of biomass can be converted into fuels and chemicals thermochemically [5,6]. The thermochemical process is divided in two stages; in the first, biomass is converted to an intermediate mixture of gases known as "synthesis gas" or "syngas" typically via gasification, in the second, syngas is catalytically converted to the final product. In the latter stage, the performance of the selected catalyst is of key importance for the overall process. Much effort has been put into designing a selective catalyst for the synthesis of ethanol from syngas. The rhodium-based catalysts are among the most selective catalysts reported in the literature [7,8]. However, few reports are found using mesoporous silica as catalyst support [9–11], although various mesoporous materials have been applied in other catalytic reactions showing interesting results [12,13]. MCM-41 is a mesoporous silica that has 1D-hexagonal porous arrangement with a pore diameter between 1.6–10 nm and a wall thickness of around 0.8 nm [14,15]. The large surface area of MCM-41, usually 1000 m^2/g or more, can be of great utility for dispersing the active sites and hence boost the catalyst activity per unit of mass. To the best of our knowledge, there is no comparison between a mesoporous Rh/MCM-41 catalyst and a typical Rh/SiO$_2$ catalyst. Ma *et al.* [9] have compared Rh-Mn/MCM-41 with Rh-Mn/SiO$_2$, however, the presence of manganese may considerably affect the reactivity of the catalysts and no direct information about the effect of MCM-41 could be inferred. Chen *et al.* [10,11] have studied the effect of metal promoters (Mn and Fe) using another type of mesoporous silica (SBA-15).

In order to evaluate the catalytic performance of Rh/MCM-41 and Rh/SiO$_2$, some considerations regarding the metal loading, degree of metal dispersion (H/Rh) and syngas conversion level must be taken. Arakawa *et al.* [16] and Underwood and Bell [17] have studied the effect of metal dispersion, from 10% to 82%, which was obtained by increasing the metal loading from 0.1% to 30% Rh. Both studies showed a large effect of the metal dispersion on the product selectivity. However, the experiments carried out by Arakawa *et al.* [16] might have been affected by secondary reactions since the syngas conversion level was not the same in all the experiments (it varied from 0.4% to 27.9% depending on the metal loading). Underwood and Bell [17] kept the syngas conversion level below 0.1%, thus reducing the risk of secondary reactions, however, the various extents of metal loading could have affected their results. Tago *et al.* [18] showed that the extent of metal loading affects the

product selectivity, according to their experiments carried out at constant H/Rh = 25% with the metal loading varied from 0.6% to 3.5% Rh. In a more recent work, Zhou *et al.* [19] used Rh/SiO_2 catalysts with different metal dispersions while keeping the same metal loading (3% Rh) testing them at low syngas conversion level (0.7%–1.5%). They observed that the degree of metal dispersion directly affects the product selectivity. Therefore, in order to avoid the effects of (i) secondary reactions; (ii) degree of metal dispersion and (iii) extent of metal loading over the product selectivity, the catalytic testing of Rh/MCM-41 and Rh/SiO_2 should be carried out at (1) low syngas conversion level; (2) equal degree of metal dispersion and (3) equal metal loading.

In the present work, we have evaluated the catalytic performance of a mesoporous Rh/MCM-41 catalyst and compared it with a typical Rh/SiO_2 catalyst. Both catalysts were tested for the synthesis of ethanol from syngas at low syngas conversion level (2.8%), same metal dispersion (H/Rh = 22%) and equal Rh loading (3 wt. %). Different product selectivities were found over Rh/MCM-41 and Rh/SiO_2. Additional experiments have been made in order to clarify the obtained results: (a) addition of water to the syngas feed-stream and (b) lowering of the syngas ratio (H_2/CO). The results from these experiments together with the catalyst characterization (BET, XPS, XRD, TEM, TPR), before and after reaction, indicate that the differences in the product selectivities can be attributed to the concentration of water vapor in the pores of Rh/MCM-41, which promote the water-gas-shift-reaction (WGSR) and produce extra CO_2 and H_2. These results confirm a previous study where high selectivity to CO_2 was observed over Rh/MCM-41 at various levels of syngas conversion as well as at different catalyst reduction temperatures [20].

2. Results and Discussion

The results obtained in the present study are divided into two sections. The first, Section 2.1., describes the catalytic performances of Rh/SiO_2 and Rh/MCM-41, which includes the effect of water addition and different syngas ratios (H_2/CO) (Section 2.1.1.). The second, Section 2.2., describes the catalysts characterization, before and after reaction, through the following techniques: N_2-physisorption (Section 2.2.1.), X-ray photoelectron spectroscopy (Section 2.2.2.), powder X-ray diffraction (Section 2.2.3.), transmission electron microscopy (Section 2.2.4.) and temperature programmed reduction (Section 2.2.5.). Finally, an interpretation of the obtained results and a discussion are then presented (Section 2.3.).

2.1. Catalytic Performances of Rh/SiO₂ and Rh/MCM-41

In order to examine the activity of the Rh/SiO_2 and Rh/MCM-41 catalysts, similar reaction conditions were used, that is reaction temperature and pressure of 280 °C and 20 bar, respectively. The gas hourly space velocity (GHSV) was varied in order to obtain a syngas conversion equal to 2.8% and the syngas ratio was equal to $H_2/CO = 2/1$. Similar conversion levels were applied for studies regarding the metal dispersion on rhodium-based catalysts [17–19]. At low syngas conversion, the occurrence of secondary reactions can be diminished and, at the same time, a uniform catalyst bed temperature can be reached. In all the experiments, the axial temperature gradient through the catalyst bed (measured by a mobile thermocouple introduced in a thermowell inside the catalyst bed) was always less than 1 °C.

Different product selectivities are obtained over Rh/SiO$_2$ and Rh/MCM-41 catalysts, as shown in Figure 1. If the selectivity toward all hydrocarbon compounds (methane and higher hydrocarbons) and the selectivity toward all oxygenated compounds (methanol, carbon dioxide, ethanol, acetaldehyde, acetic acid, methyl acetate and ethyl acetate) are considered in Figure 1, the following results are obtained: 58.2% hydrocarbon compounds and 41.8% oxygenated compounds for Rh/SiO$_2$, while for Rh/MCM-41 results 43.4% hydrocarbon compounds and 56.6% oxygenated compounds. This indicates that more hydrocarbon compounds are formed in Rh/SiO$_2$ than in Rh/MCM-41. Underwood and Bell have used a Rh/SiO$_2$ catalyst with a similar metal dispersion to the one used in our study (H/Rh = 10%) and also found a higher selectivity to hydrocarbons than to oxygenates [17].
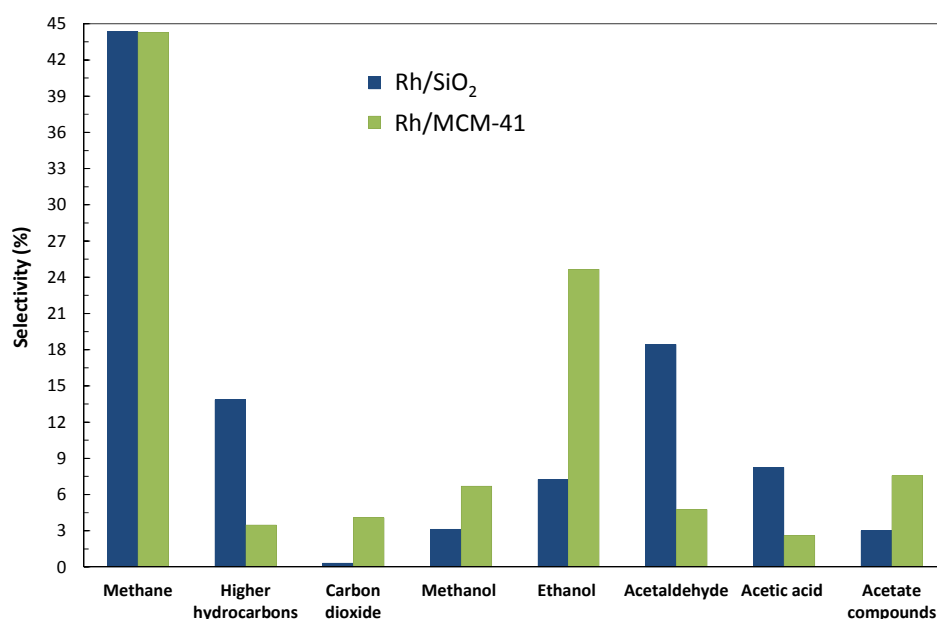
Figure 1. Product selectivities obtained from the conversion of syngas over Rh/SiO$_2$ and Rh/MCM-41. Higher hydrocarbons: ethane, propane and butane. Acetate compounds: methyl acetate and ethyl acetate. Reaction conditions: 280 °C, 20 bar, GHSV = 12,000 mL$_{syngas}$/g$_{cat}$·h for Rh/SiO$_2$ and GHSV = 3000 mL$_{syngas}$/g$_{cat}$·h for Rh/MCM-41.

Table 1. Selectivity to C$_2$-oxygenated compounds (ethanol, acetaldehyde and acetic acid) at different syngas ratios (H$_2$/CO) and with/without addition of water. Temperature of 280 °C and pressure of 20 bar.

Catalyst	Syngas Ratio H$_2$/CO	GHSV (mL/g·h)	Conversion (%)	TOF (s^{-1})	Total Selectivity to C$_2$-oxygenated (%)	Selectivity between C$_2$-oxygenated. (%)		
						Ethanol (%)	Acetaldehyde (%)	Acetic Acid (%)
Rh/SiO$_2$	2/1	12000	2.8	0.039	34	21	54	24
	2/1 *	6000	1.6	0.011	18	8	83	9
	1/1	6000	2.1	0.022	32	16	51	34
Rh/MCM-41	2/1	3000	2.8	0.010	32	77	15	8
	2/1 *	3000	1.0	0.005	1	65	35	0
	1/1	3000	0.4	0.002	35	69	10	21

* Water added.

Regarding the formation of the C_2-oxygenated compounds (ethanol, acetaldehyde and acetic acid), it can be seen from Table 1 (syngas ratio $H_2/CO = 2/1$) that the selectivity trend for Rh/SiO_2 decreases in the following order: acetaldehyde > acetic acid > ethanol. While for Rh/MCM-41 it decreases as: ethanol > acetaldehyde > acetic acid. Interestingly, the total selectivity to C_2-oxygenated compounds is similar in both catalysts; 34% for Rh/SiO_2 and 32% for Rh/MCM-41.

2.1.1. Addition of Water Vapor and Lower Syngas Ratio ($H_2/CO = 1/1$)

Figure 2 shows the effect of the addition of water to the syngas feed-stream for Rh/SiO_2 and Rh/MCM-41 catalysts. The addition of water vapor decreases the syngas conversion from 2.8% to 1.0% for Rh/MCM-41 at GHSV = 3000 $mL_{syngas}/g_{cat} \cdot h$. For Rh/SiO_2, since a very low syngas conversion was found at GHSV = 12,000 $mL_{Syngas}/g_{cat} \cdot h$, it was necessary to decrease the space velocity to GHSV = 3000 $mL_{syngas}/g_{cat} \cdot h$ to achieve a syngas conversion of 1.6%, which indicates a considerable decrease of the activity for Rh/SiO_2 in the presence of water vapor. It can also be observed that the addition of water notably increases the selectivity to CO_2 in both catalysts; from 0.3% to 18.5% for Rh/SiO_2 and from 4.1% to 90.4% for Rh/MCM-41. Likewise, while the selectivity to the rest of the products is reduced in both catalysts, the selectivity to methanol is considerably increased over Rh/SiO_2, but it is somewhat reduced over Rh/MCM-41. Finally, the total selectivity to C_2-oxygenated compounds is notably reduced in both catalysts, as can be seen in Table 1 (syngas ratio $H_2/CO = 2/1$ *), being more marked in Rh/MCM-41. Moreover, the selectivity trends are kept in the same order for Rh/SiO_2 (acetaldehyde > acetic acid > ethanol) and for Rh/MCM-41 (ethanol > acetaldehyde > acetic acid) as in the experiments without water addition (Table 1).
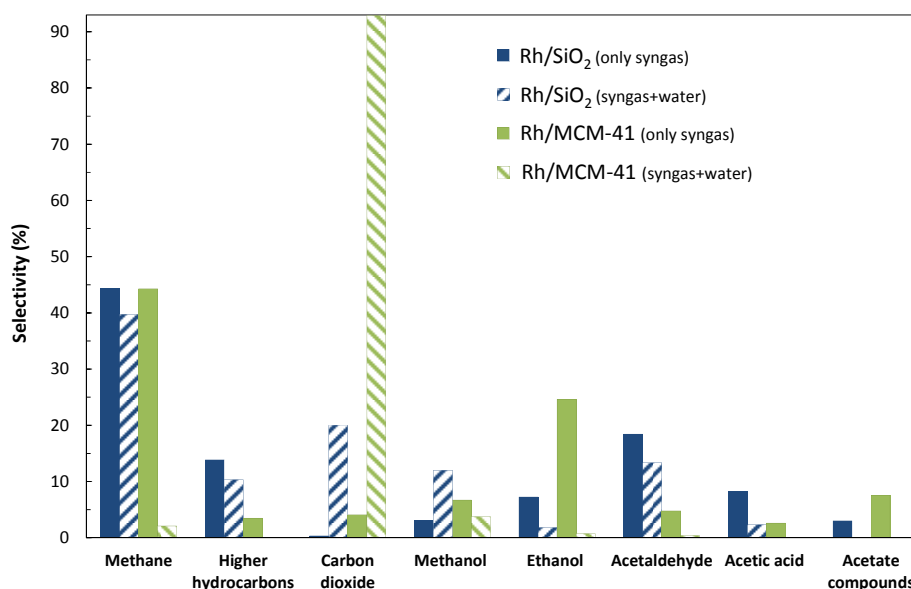
Figure 2. Comparison of the product selectivities obtained from the conversion of syngas with and without addition of water over Rh/SiO_2 and Rh/MCM-41. Reaction conditions (with addition of water): 280 °C, 20 bar, GHSV = 6000 $mL_{syngas}/g_{cat} \cdot h$ ($H_2:CO:H_2O$ = 2:1:2.7) for Rh/SiO_2 and GHSV = 3000 $mL_{syngas}/g_{cat} \cdot h$ ($H_2:CO:H_2O$ = 2:1:1.5) for Rh/MCM-41. Reaction conditions for the experiments without addition of water as indicated in Figure 1.

Figure 3 shows the effect of changing the syngas ratio from $H_2/CO = 2/1$ to $H_2/CO = 1/1$ for Rh/SiO$_2$ and Rh/MCM-41 catalysts. The lowering of syngas ratio from $H_2/CO = 2$ to $H_2/CO = 1$ decreases the syngas conversion in both catalysts; from 2.8% to 0.4% for Rh/MCM-41 at GHSV = 3000 mL$_{syngas}$/g$_{cat}$·h and from 2.8% (GHSV = 12,000 mL$_{syngas}$/g$_{cat}$·h) to 2.1% (GHSV = 6000 mL$_{syngas}$/g$_{cat}$·h) for Rh/SiO$_2$. The reduction of the syngas conversion by the lowering the syngas ratio has also reported in the literature, which is attributable to a lesser extent of the hydrogenation reactions (hydrocarbon formation) [7,8].

In both catalysts, the lowering of the syngas ratio results in less production of methane and methanol while, in contrast, more higher hydrocarbons, carbon dioxide, and acetate compounds are obtained (Figure 3). When the syngas H_2/CO ratio is lowered, the partial pressure of hydrogen is expected to be decreased. This suggests that the products with high H/C ratios, such as CH$_4$ and CH$_3$OH, could be favored at high partial pressure of hydrogen (high syngas H_2/CO ratio). Likewise, the products with lower H/C ratios, such as the higher hydrocarbons and oxygenated compounds could be favored at low partial pressure of hydrogen (low syngas H_2/CO ratio). These results are in agreement with the literature regarding the effect of the syngas ratio for rhodium-based catalysts [7,8]. In addition, among the C$_2$-oxygenated compounds it can be observed that the selectivity to acetic acid is favored at low syngas H_2/CO ratio, while the selectivities to the more hydrogenated compounds (ethanol and acetaldehyde) are favored at higher syngas H_2/CO ratio, as is observed in Table 1 (see syngas ratio $H_2/CO = 2/1$ and $H_2/CO = 1/1$).
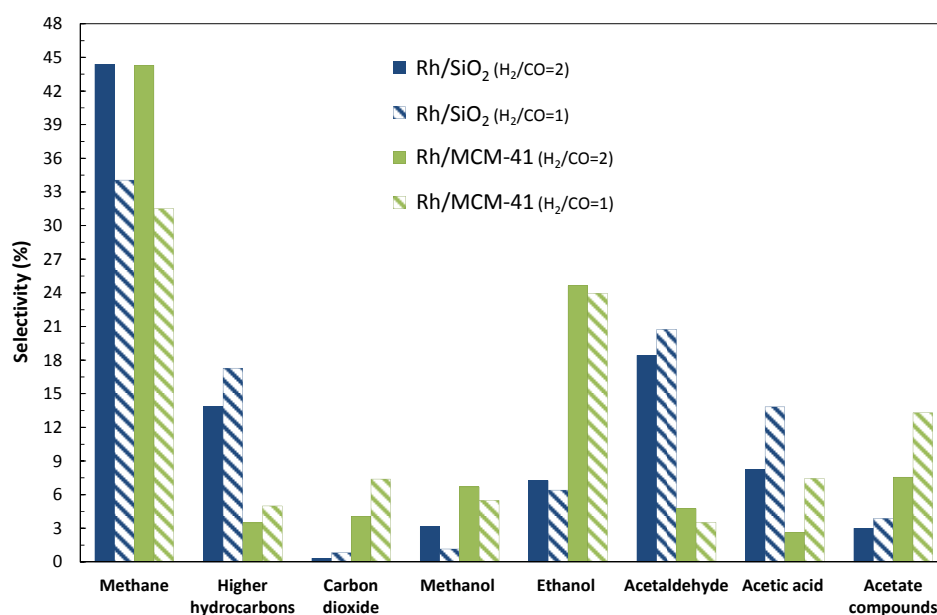
Figure 3. Comparison of the product selectivities obtained from the conversion of syngas with $H_2/CO = 2$ and $H_2/CO = 1$ over Rh/SiO$_2$ and Rh/MCM-41. Reaction conditions (syngas $H_2/CO = 1$): 280 °C, 20 bar, GHSV = 6000 mL$_{syngas}$/g$_{cat}$·h for Rh/SiO$_2$ and GHSV = 3000 mL$_{syngas}$/g$_{cat}$·h for Rh/MCM-41. Reaction conditions for the experiments with syngas $H_2/CO = 2$ as indicated in Figure 1.

In a previous study a high selectivity to CO$_2$ in the Rh/MCM-41 catalyst was also observed, it was found to be independent of the catalyst reduction temperature and the syngas conversion level [20].

Figures 4 and 5 show the product selectivities and the syngas conversion with time on stream at different reaction conditions for the Rh/SiO₂ and MCM-41 catalysts, respectively. It can be noted that almost no CO_2 is formed over the Rh/SiO₂ catalyst (Figure 4, Period A–F) whatever the reaction condition (T, P, GHSV) or catalyst reduction temperature (200, 370, 500 °C and non-reduced) applied. On the other hand, a high selectivity to CO_2 is observed over the MCM-41 catalyst at all reaction conditions studied and at different catalyst reduction temperatures (Figure 5, Period A'−G'). Thus, the product selectivity is notably affected by the MCM-41 support in a large range of reaction conditions and at different catalyst reduction temperatures. These results together with the catalysts characterization (Section 2.2) are discussed later on in Section 2.3.
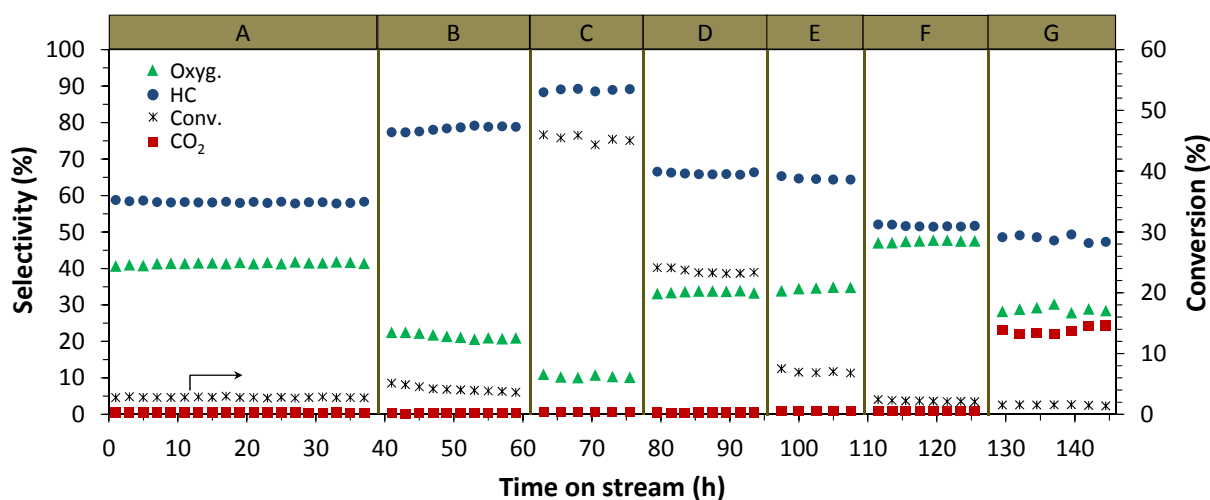
Figure 4. Selectivities and conversion with time on stream for the Rh/SiO₂ catalyst. Oxyg.: alcohols, acetaldehyde, acetic acid and esters. HC: methane and higher hydrocarbons. See Table S1 in supporting information for details about the reaction conditions in periods A–G.
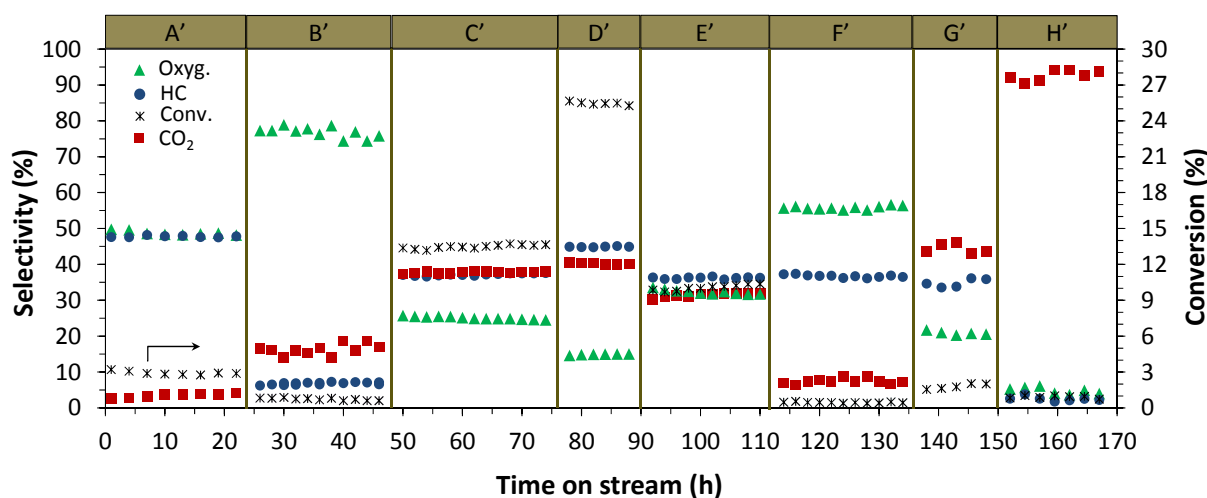
Figure 5. Selectivities and conversion with time on stream for the Rh/MCM-41 catalyst. Oxyg.: alcohols, acetaldehyde, acetic acid and esters. HC: methane and higher hydrocarbons. See Table S1 in supporting information for details about the reaction conditions in periods A'–H'.

2.2. Catalyst Characterization

2.2.1. N_2-Physisorption

In Table 2 the results obtained from N_2-physisorption are reported. When comparing the pure supports, the surface area of MCM-41 is about four times larger than the surface area of SiO_2. A similar relation is observed when 3 wt. % Rh is impregnated in both supports. This indicates that the process of rhodium incorporation (aqueous impregnation, drying and calcination) affects to a similar extent the surface area of MCM-41 and the surface area of SiO_2. In some reported studies, the surface area of MCM-41 is drastically affected by metal incorporation: for example, the impregnation with 5wt. % Co reduced the original MCM-41 surface area by nearly 50% [21]. However, the incorporation of Rh into MCM-41 only reduces the original MCM-41 surface area by 0.9%, as shown in Table 2. After catalytic testing, the surface area was reduced by 3.7% for Rh/SiO_2 and 9.0% for Rh/MCM-41. More notable changes are observed when water is added to the syngas feed-stream, then the surface areas of Rh/SiO_2 and Rh/MCM-41 are reduced by 10.3% and 19.3%, respectively (Table 2). The more significant effect of water on the surface area of Rh/MCM-41 is consistent with the structure degradation of mesoporous materials proposed by Landau *et al.* [22]. Therefore, the hydration of the siloxane structure is followed by siloxane hydrolysis-hydroxylation and their rearrangement-redehydroxylation during calcination. This results in a few 1D-channels collapsing into a single one [22]. As a consequence, there is a loss of Bragg intensity (as will be evidenced by XRD analysis, Figure 6), decreasing the pore volume (as observed in Table 2), while retaining uniform pore size (as described below and further shown by TEM analysis, Figure 7).

Regarding the pore size distribution of Rh/SiO_2 and Rh/MCM-41 (see Figure S1 in supporting information) confirmed, a wide pore size distribution is observed in the pure SiO_2, which is narrowed after Rh impregnation. Pure MCM-41 presents a narrow pore size distribution and smaller pore sizes as compared to SiO_2; after Rh impregnation no significant changes are observed. From the adsorption isotherms, the average pore size of Rh/SiO_2 is much larger than in the case of Rh/MCM-41; 19 nm and 2.5 nm, respectively. Finally, after catalytic testing (with and without water) there is no significant change in the pore size distribution for any of the catalysts.

2.2.2. X-ray Photoelectron Spectroscopy (XPS)

In Table 2, the results from XPS analysis are summarized. Before the catalytic testing, we can observe that the oxidation state of Rh is similar in both Rh/SiO_2 and Rh/MCM-41 catalysts. After the catalytic testing (without addition of water), the fraction of Rh^{3+} is increased in Rh/SiO_2 while it is decreased in Rh/MCM-41. After the catalytic testing with addition of water, all Rh species are in the form of Rh^0 in both catalysts. Finally, the Rh/Si ratio indicates that Rh species migrate to the surface of the catalysts as a consequence of the catalytic testing. The latter phenomenon is more pronounced when water is added to the catalytic system.

Table 2. N₂-physisorption and XPS analyses of the Rh/SiO₂ and Rh/MCM-41 catalysts, before and after the catalytic testing.

Catalyst	Condition	Surface Area (m²/g)	Change in Surface Area	Pore Volume (cm³/g)	Rh⁰		Rh³⁺		Rh/Si
					%	Binding energy (eV)	%	Binding energy (eV)	
Rh/SiO₂	Pure support	238	-	0.87	-	-	-	-	-
	Before catalytic testing	236	0.5% *	0.90	86.5	307.3	13.4	309.7	0.0057
	After catalytic testing (280 °C, 20 bar, 12,000 mL/g·h): *only syngas*	228	3.7% **	0.90	82.4	307.3	17.6	309.7	0.0064
	After catalytic testing (280 °C, 20 bar, 6000 mL/g h): *syngas and water*	212	10.3% **	0.88	100	307.2	-	-	0.0079
Rh/ MCM-41	Pure support	970	-	1.08	-	-	-	-	-
	Before catalytic testing	961	0.9% *	1.15	80.6	307.1	19.4	308.6	0.0079
	After catalytic testing (280 °C, 20 bar, 3000 mL/g·h): *only syngas*	875	9.0% **	1.04	90.8	307.4	9.2	309.3	0.0087
	After catalytic testing (280 °C, 20 bar, 3000 mL/g·h): *syngas and water*	776	19.3% **	0.94	100	307.1	-	-	0.0100

* Compared to the pure support. ** Compared to the catalyst before catalytic testing.

2.2.3. Powder X-ray Diffraction (XRD)

Mesoporous MCM-41 has characteristic signals at small-angle XRD, which are indicated in Figure 6 as (100), (110), and (200) reflections. These signals correspond to a hexagonal structure with unit cell parameter $a = 2d_{100}/\sqrt{3}$ [14]. An additional (210) reflection is reported in the literature, which gives a low intensity signal at around 2θ = 5.9 [14]. In qualitative terms, the intensity of the XRD signals can be attributed to the long-range periodic structure of MCM-41 [21]. Although the long-range ordering in Rh/MCM-41 decreases after impregnation with Rh (Figure 6A) and after catalytic testing (Figure 6B,C), it does not completely disappear. In addition, it can be observed that all signals appear at the same 2θ, *i.e.*, same d-spacing, which suggests that there is no significant lattice contraction either after Rh impregnation or after catalytic testing. Typical SiO₂ support does not present a pore ordering as mesoporous MCM-41, thus no signals are found at small-angle XRD (Figure 6). The wide-angle XRD patterns in Figure 6 indicate that both catalysts Rh/SiO₂ and Rh/MCM-41 are amorphous materials. It also indicates that there is no segregation of rhodium oxides (or at least they are not large enough to be detected by the XRD technique) after impregnation with Rh

(Figure 6A) and after catalytic testing without addition of water (Figure 6B). After catalytic testing with addition of water (Figure 6C) a low-intensity and broad signal appears at around $2\theta = 35$–40. This range of 2θ corresponds to the characteristic signals of Rh_2O_3 and Rh^0. According to the XPS analysis, all Rh species are converted to Rh^0 when water is added to the catalytic system. Therefore, we can conclude that the presence of water in the syngas feed-stream slightly favors the growth of Rh^0 clusters.
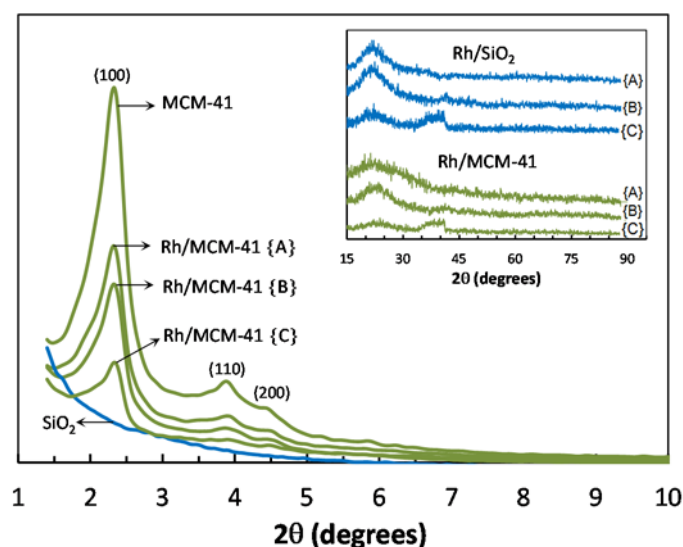
Figure 6. Small and wide angle XRD patterns of pure supports SiO_2 and MCM-41, impregnated with Rh (**A**); after catalytic testing (**B**); and after catalytic testing with addition of water (**C**). Catalytic testing at same conditions as indicated in Table 2.

2.2.4. Transmission Electron Microscopy (TEM)

In Figure 7, TEM images for Rh/SiO_2 and Rh/MCM-41 catalysts are shown. Before reaction, the average Rh particle size is similar in both catalysts; 4 nm for Rh/SiO_2 and 3 nm for Rh/MCM-41. Which agrees with the average metal particle size equal to 4 nm derived from the metal dispersion (H/Rh = 22%), assuming an icosahedral particle shape [23]. For the Rh/SiO_2 catalyst, the average Rh particle size has grown after the catalytic testing (with and without water). Less effect is observed for the Rh/MCM-41 catalyst, where the average particle size is kept to 3 nm after the catalytic testing, even with addition of water. It can be noted that the pore diameter of MCM-41 is in the same range as the Rh particle size in the Rh/MCM-41 catalyst (Figure 7A-Rh/MCM-41), it may suggest that the pore diameter of MCM-41 limits the growth of Rh particles. This is supported by Zhou *et al.* [19] who observed a relation between the Rh particle size and the pore diameter in various silica supports. If it is so, it could explain the narrow Rh particle size distribution in the mesoporous Rh/MCM-41 catalyst, even after the catalytic testing (Figure 7B,C-Rh/MCM-41), as compared to the particle size distribution in the Rh/SiO_2 catalyst (Figure 7A–C-Rh/SiO_2).

From XRD analysis (Figure 6), after the catalytic testing (with addition of water) a new and broad signal is observed in both catalysts. This signal corresponds to Rh^0 according to XPS (Table 2). For the Rh/SiO_2 catalyst, these results agree with the growth of the particle size observed in TEM images (Figure 7). For the Rh/MCM-41 catalyst, it seems that the pores of MCM-41 support limit the growth of Rh

and thus the particle size distribution is little affected. Possibly, the signal detected in XRD for Rh/MCM-41 may be due mostly to an increased number of Rh^0 dispersed along the pores.
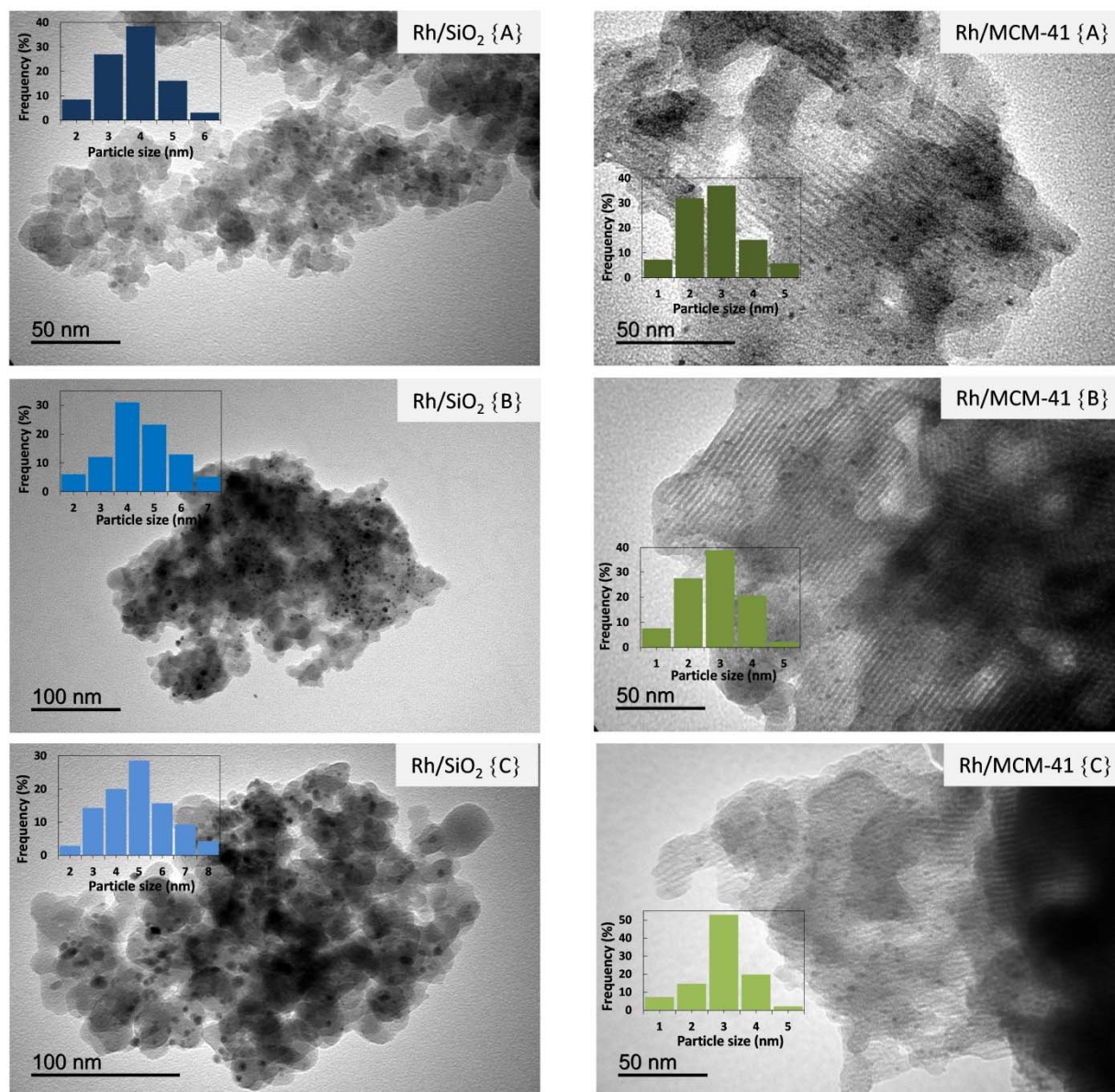
Figure 7. TEM images of Rh/SiO₂ and Rh/MCM-41 catalysts; reduced (**A**); after catalytic testing (**B**); and after catalytic testing with addition of water (**C**). Catalytic testing at same conditions as indicated in Table 2.

2.2.5. Temperature Programmed Reduction (TPR)

Figure 8 shows the TPR profiles for the Rh/SiO₂ and Rh/MCM-41 catalysts. It can be seen that the reduction of rhodium oxide species begins at low temperatures, in agreement with the literature [24,25]. All Rh species seem to be reduced at temperatures below 200 °C. The TPR profile of the Rh/MCM-41 catalyst suggests some metal-support interactions, which widen the reduction peak at higher temperatures. Metal-support interactions are observed in other mesoporous catalysts as well as in traditional catalysts [13,26]. Moreover, after the reduction treatment at 370 °C the surface of the

Rh/SiO$_2$ and Rh/MCM-41 catalysts are composed of a similar proportion of Rh^0 and Rh^{3+}, as is indicated by XPS analysis (Section 2.2.2.).
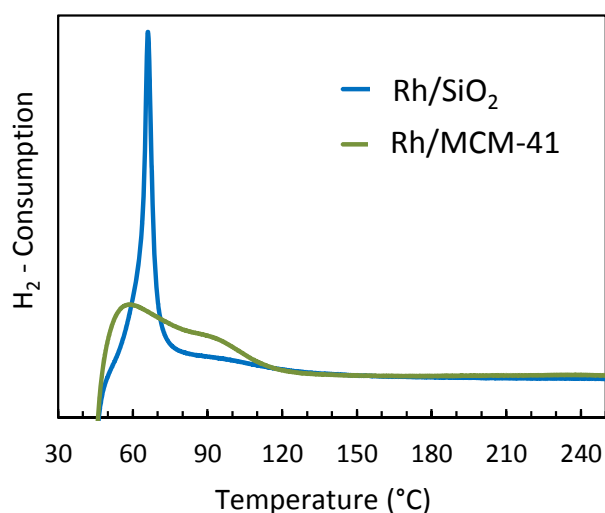
Figure 8. Temperature programmed reduction profiles of the Rh/SiO$_2$ and Rh/MCM-41 catalysts.

2.3. Interpretation of the Catalytic Performance of Rh/MCM-41 Compared to Rh/SiO$_2$

As observed in Figure 1, the product selectivity obtained for the conversion of syngas over Rh/MCM-41 is notably different compared to the product selectivity found over Rh/SiO$_2$. These differences can be due to the different characteristics of the supports: MCM-41 and SiO$_2$. It may be that the 1D-channels with small pore diameter of MCM-41, which seem to be retained in Rh/MCM-41 (as suggested from N$_2$-physisorption, XRD and TEM analyses), could affect the catalytic performance when comparing with a typical SiO$_2$ support which has large and non-ordered pore diameters. Another characteristic is the metal-support interactions in Rh/MCM-41, which seems to be absent in Rh/SiO$_2$ (as suggested from TPR analysis). However, the later characteristic may not be important during the catalytic testing since the final surface composition is similar in both catalysts (as indicated from XPS analysis). The product selectivity could neither have been affected by the Rh particle size because, on the one hand, both catalysts have been pre-reduced at conditions to obtain similar metal dispersion (*i.e.*, similar metal particle size, which is confirmed by TEM images). On the other hand, we cannot relate the slight growth of the Rh particle size in the Rh/SiO$_2$ catalyst with the increased selectivity to CO$_2$ (approx. 20%), because, if this would be the case, the selectivity to CO$_2$ in the Rh/MCM-41 catalyst should be less than 20% since the growth of the Rh particle size is even lower for this catalyst (as shown the TEM images), but its selectivity to CO$_2$ is above 90%.

It has been suggested that a high concentration of water vapor can be formed in the pores of MCM-41 during catalyst reduction, which could promote metal-support interactions [13,27]. If so, water vapor can also be concentrated in the catalyst pores during catalytic testing, since most of the syngas reactions produce water as a main by-product (reactions 1–4) [7,8]. As a consequence, an environment rich in water vapor can be formed which may induce some reactions, such as the water-gas-shift-reaction (WGSR). WGSR generates extra carbon dioxide and hydrogen (reaction 5). In concordance, more

carbon dioxide is produced by Rh/MCM-41 than by Rh/SiO2 (see Figure 1). Hydrogen was unfortunately not measured due to analytical limitations since hydrogen has similar thermal conductivity to the carrier helium in the GC analysis. However, if we consider the selectivity towards the C2-oxygenated compounds (Table 1), the selectivity to the more hydrogenated compounds, *i.e.*, ethanol and acetaldehyde, accounts for 92% over Rh/MCM-41, while it is only 75% over Rh/SiO2. This may suggest that the extra hydrogen generated from the WGSR over Rh/MCM-41 would facilitate the hydrogenation of acetic acid (or a C2-oxygenated intermediary, perhaps an acetyl intermediate [28]) to acetaldehyde and ethanol.

$$\text{Ethanol generation } 2CO + 4H_2 \rightarrow C_2H_5OH + H_2O : \Delta H_{298}^\circ = -253.6 \text{ kJ/mol} \tag{1}$$

$$\text{Methanation } CO + 3H_2 \rightarrow CH_4 + H_2O : \Delta H_{298}^\circ = -205.9 \text{ kJ/mol} \tag{2}$$

$$\text{Hydrocarbons formation } CO + 2H_2 \rightarrow -CH_2- + H_2O : \Delta H_{298}^\circ = -165 \text{ kJ/mol} \tag{3}$$

$$\text{Methanol synthesis } CO_2 + 3H_2 \rightarrow CH_3OH + H_2O : \Delta H_{298}^\circ = -49.7 \text{ kJ/mol } CO +$$
$$2H_2 \rightarrow CH_3OH : \Delta H_{298}^\circ = -90.5 \text{ kJ/mol} \tag{4}$$

$$\text{Water gas shift reaction } CO + H_2O \rightarrow CO_2 + H_2 : \Delta H_{298}^\circ = -41.1 \text{ kJ/mol} \tag{5}$$
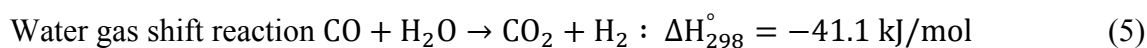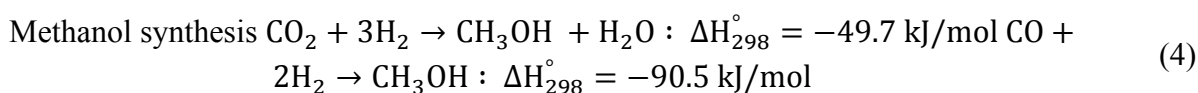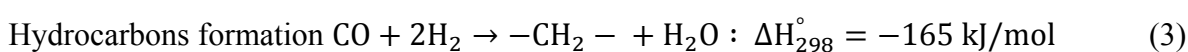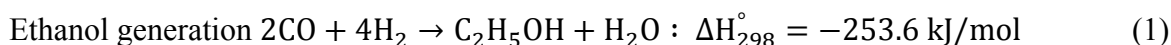
In accordance with this view, the WGSR should also be promoted over the Rh/SiO2 catalyst if water were to be concentrated in the catalyst particle. In effect, when water is added to the syngas feed-stream (Figures 2 and 4) the selectivity to CO2 is enhanced from almost zero to approximately 20%. In the case of the Rh/MCM-41 catalyst, an even higher concentration of water is obtained in the 1-D channel pores, boosting the selectivity to CO2 (>90%). This means that the WGSR is highly favored in the presence of water, whatever kind of silica support is used, SiO2 or MCM-41. In the presence of water vapor, all Rh species are in the form of Rh^0 (as suggested by XPS analysis). Still there is no agreement in the literature on which Rh species (Rh^0, Rh^{n+}) is more active for the oxygenate formation. Chuang *et al.* [29] suggest that Rh^0 is less active than the oxidized form. Our results might support this idea since the lowest activities found in both catalysts occurred when both catalysts had 100% Rh^0. At the same time, as CO2 is produced by the addition of water in both catalysts, the selectivity to methanol is increased in Rh/SiO2 (Figure 2). For Rh/MCM-41, although the selectivity to methanol is somewhat reduced by the addition of water, it is not as drastically reduced as the selectivity to the rest of products (Figure 2). Therefore, it seems that the formation of CO2 and methanol is favored in the presence of water, where the WGSR would play an important role. Indeed, it is generally accepted that the synthesis of methanol from syngas occurs primary via the hydrogenation of CO2 [30]. This means that the occurrence of the WGSR, as a consequence of the concentration of water vapor in Rh/MCM-41, may contribute to the generation of methanol from CO2, which may explain the higher selectivity to methanol observed in Rh/MCM-41 compared to Rh/SiO2 (Figure 1).

Regarding the effect of the hydrogen partial pressure on the selectivity to the C2-oxygenated compounds, when it decreases, the selectivity towards acetic acid should increase in both catalysts. It can be observed that when changing the syngas ratio from H2/CO = 2/1 to H2/CO = 1/1 (Table 1), more acetic acid is evidently formed in both catalysts. This may also support the idea that WGSR occurs in Rh/MCM-41 producing extra H2, which may facilitate the hydrogenation of acetic acid (or a C2-oxygenated intermediary) yielding more acetaldehyde and ethanol than in the typical Rh/SiO2

catalyst (Table 1). Furthermore, the product distribution between the C_2-oxygenates in Rh/MCM-41 always keeps the relation according to the extent of oxidation of each compound: ethanol > acetaldehyde > acetic acid (Figures 1–3).

The reaction mechanism for the conversion of syngas to oxygenated compounds over rhodium-based catalyst, is not fully understood [7,8,28]. For example, it is suggested that acetate compounds can be formed by the reaction of CO_2 with surface intermediates such as CH_x* species [31]. If this reaction occurs over Rh/SiO$_2$ and Rh/MCM-41, the additional formation of CO_2 via WGSR in Rh/MCM-41 would consume much more CH_x* species than in Rh/SiO$_2$. This means that a lesser number of CH_x* species would be available for conversion into hydrocarbon compounds and more acetate compounds should be expected in the Rh/MCM-41 catalyst. This is in accordance with our results, since lower selectivity to hydrocarbon compounds and higher selectivity to acetate compounds are found over Rh/MCM-41 as compared to Rh/SiO$_2$ (Figure 1). However, we must indicate that the discussion of the elementary steps or reaction mechanism for ethanol formation is not the objective of this work, we rather study the performance of a Rh/MCM-41 catalyst. Studies such as micro-kinetics together with theoretical calculations can be helpful for a fundamental understanding of the reaction mechanism. Very interesting reports on this topic have been published in recent years [32,33]. The inclusion of the WGSR and its effect on the product distribution can be interesting to study and compare with the results obtained in the present work.

From the above discussion, we believe that the differences in activity and selectivity observed for Rh/SiO$_2$ and Rh/MCM-41 are highly related to the concentration of water vapor in Rh/MCM-41. This is also supported by a previous investigation where high selectivity to CO_2 was found over the mesoporous Rh/MCM-41 catalyst at various levels of syngas conversion as well as at different catalyst reduction temperatures [20] (Figures 4 and 5). The metal-support interactions in Rh/MCM-41 might contribute to the observed differences, but probably to a much lower extent than the effect of water vapor. In summary, the high concentration of water vapor in the pores of Rh/MCM-41 may promote the occurrence of the WGSR, generating extra CO_2 and H_2, which in turn facilitate side reactions changing the product selectivity. Finally, it seems that, as a consequence of the extra hydrogen generated from the WGSR in Rh/MCM-41, more acetaldehyde and/or acetic acid (or a C_2-oxygenated intermediary) is hydrogenated yielding more ethanol than in the typical Rh/SiO$_2$ catalyst.

3. Experimental Section

3.1. Catalyst Preparation and Characterization Techniques

Hexagonal mesoporous silica (MCM-41) is usually obtained by the "atrane route" [34]. In this method, cetyltrimethylammonium bromide is used as the structural directing agent, and triethanolamine (TEA) is used as a hydrolysis retarding agent. Silatrane complexes are formed between tetraethyl orthosilicate and TEA, as metal precursors of Si. Further preparation procedure has been described elsewhere [34,35]. A commercial MCM-41 from Sigma Aldrich (Sigma Aldrich, St. Louis, MO, USA) was indistinctly used to the MCM-41 obtained from the "atrane route". Silica (SiO$_2$) catalyst support was purchased from Alfa Aesar (Alfa Aesar, Karlsruhe, Germany). The Rh/MCM-41 and Rh/SiO$_2$ catalysts were prepared by successive incipient wetness impregnation, using an aqueous

solution of $RhCl_3 \cdot nH_2O$. After impregnation, the catalysts were dried and then calcined at 500 °C/5 h. The total metal loading was 3 wt. % Rh for both Rh/MCM-41 and Rh/SiO$_2$ catalysts.

Powder X-ray diffraction (XRD) was performed using a Siemens D5000 instrument (Siemens, Karlsruhe, Germany) with Cu K-α radiation (2θ = 10°–90°, step size = 0.04°) equipped with a Ni filter and operated at 40 kV and 30 mA. N$_2$-physisorption was carried out using a Micromeritics ASAP 2000 instrument (Micromeritics, Norcross, GA, USA). The Brunauer-Emmett-Teller (BET) method was used to calculate the surface area and the Barrett-Joyner-Halenda (BJH) method was used to calculate the pore size and pore volume from the desorption isotherm. Temperature programmed reduction (TPR) was carried out in a Micromeritics Autochem 2910 instrument (Micromeritics, Norcross, GA, USA), a reducing gas mixture (5% H$_2$ in Ar) at a flow of 50 mL/min passed through the catalyst sample while the temperature was increased by 5 °C/min up to 900 °C. Transmission electron microscopy (TEM) images were obtained using a JEOL JEM 1400 microscope (JEOL, Tokio, Japan). Samples were mounted on 3 mm holey carbon copper grids. Particle size and distribution were estimated after examination of more than 100 metal particles.

The metal dispersion was measured by H$_2$-chemisorption using a Micromeritics ASAP 2020 instrument (Micromeritics, Norcross, GA, USA). Prior to the analysis, the catalyst sample was reduced with hydrogen. After vacuum evacuation, a dynamic mode of hydrogen injection was performed at 40 °C [36]. Repeated analyses were made in order to discriminate between the amount of hydrogen adsorbed via physisorption or chemisorption [37]. The stoichiometry of hydrogen chemisorbed on metallic rhodium was considered to be 1:1. Different degrees of metal dispersion were obtained by changing the reduction temperature and the reduction time. In order to obtain the same metal dispersion, the catalysts were reduced at 370 °C during 1h for Rh/MCM-41 and 6 h for Rh/SiO$_2$, resulting in H/Rh = 22% in both catalysts.

X-ray photoelectron spectroscopy (SPECS, Berlin, Germany) data were recorded on 4 mm × 4 mm pellets of 0.5 mm thickness that were obtained by gently pressing the powdered materials, following outgassing to a pressure below 2×10^{-8} Torr at 150 °C in the instrument pre-chamber to remove chemisorbed volatile species. The main chamber of a Leybold-Heraeus LHS10 spectrometer was used, capable of operating down of 2×10^{-9} Torr, which was equipped with an EA-200MCD hemispherical electron analyzer with a dual X-ray source using AlKα (hν = 1486.6 eV) at 120 W, 30 mA, with C(1s) as energy reference (284.6 eV). The catalyst samples were analyzed as; (i) reduced at the same conditions as in the catalytic testing; (ii) after catalytic testing and; (iii) after catalytic testing with addition of water. The reaction conditions are indicated in Table 2.

3.2. Catalytic Testing

The experiments were carried out in a stainless-steel, down-flow fixed bed reactor. The system components and the on-line gas chromatograph (GC) analysis are similar to those described by Andersson *et al.* [38]. The internal diameter of the reactor was 8.3 mm, in which about 300 mg of catalyst was charged with a particle size between 160 and 250 μm. Before reaction, the catalysts were reduced following the same procedure as the H$_2$-chemisorption described above, in order to obtain a metal dispersion of H/Rh = 22%. After reduction, the reactor was cooled to 280 °C and pressurized with syngas up to 20 bar. The gas hourly space velocity (GHSV) was varied between 3000–19,000

mL_{syngas}/g_{cat}. Premixed syngas bottles (AGA Linde) with a H_2/CO ratio of 2:1 and 1:1 were used. The amount of water added to the system was regulated by means of a Gilson 307 pump, then the dosed water was evaporated by an external tape heater at 225 °C and then mixed with the syngas feed-stream.

An on-line GC Agilent 7890A (Agilent, Santa Clara, CA, USA) was used to quantify the reaction products. A detailed description of the GC configuration and the analytical procedure have been published previously by Andersson *et al.* [38]. N_2 added to the syngas mixture was used as internal standard to quantify CH_4, CO and CO_2 in a thermal conductivity detector [39]. The internal normalization of corrected peak areas was used to quantify the hydrocarbon and oxygenated compounds in a flame ionization detector [39]. The expressions used to calculate the syngas conversion, carbon mole selectivity and carbon balance are reported in [38]. In all the experiments the carbon balance was in the range of 99.1%–100%.

Preliminary estimations were carried out to ascertain transport effects on the Rh/MCM-41 catalyst. At the experimental conditions used in this study, intraparticle diffusion limitation might slightly initiate at high syngas conversion (>70% in term of CO conversion), according to Weisz-Prater's criterion [40]. However, a proper estimation of the diffusion limitation would require a careful determination of the morphology of the Rh/MCM-41 catalyst, which is outside the scope of the present study. The Koros-Nowak criterion indicates that the reaction rate, in the kinetic regime, is directly proportional to the concentration of the active material [40]. This means that the turnover frequency (TOF, s^{-1}) must be invariant as the concentration of the active material is changed. An experimental test was carried out at 230 °C, 20 bar and 40,000 mL_{syngas}/g_{cat} h ($H_2/CO = 2/1$) using a catalyst sample with a fixed number of active sites (3 wt. % Rh and metal dispersion of H/Rh = 22%). A fraction of this sample was diluted with pure MCM-41 support at a ratio of 1:3, resulting in a catalyst with nominal composition 0.75 wt.% Rh and a metal dispersion of H/Rh = 22%. A minor variation (<10%) was observed between the TOFs of the non-diluted catalyst and the diluted catalyst, suggesting that the reaction operates in the kinetic regime.

4. Conclusions

The catalytic performance of Rh/MCM-41 catalyst has been evaluated for the synthesis of ethanol from syngas and compared with a typical Rh/SiO$_2$ catalyst. Equal reaction conditions have been applied (280 °C and 20 bar), low syngas conversion (2.8%), the same metal dispersion (H/Rh = 22%) and the same Rh loading (3 wt. %). Under these conditions, different product selectivities have been obtained for Rh/SiO$_2$ and Rh/MCM-41 catalysts. In order to clarify the obtained results, additional experiments were conducted: addition of water to the syngas feed-stream and lowering of the syngas ratio (H_2/CO). The results from these experiments together with the catalyst characterization, before and after reaction, indicate that the differences in the catalytic performances of Rh/SiO$_2$ and Rh/MCM-41 can be attributed to a high concentration of water vapor in the pores of Rh/MCM-41, which seem not to occur in Rh/SiO$_2$. The concentration of water vapor in Rh/MCM-41 could essentially promote the occurrence of the water-gas-shift-reaction (WGSR) which generates some extra carbon dioxide and hydrogen. The extra carbon dioxide and hydrogen could induce side reactions and thus change the product selectivity, as compared with Rh/SiO$_2$. The extra hydrogen generated from the WGSR in Rh/MCM-41 could possibly facilitate the hydrogenation of acetic acid and/or acetaldehyde (or a

C_2-oxygenated intermediary) to ethanol, which may be related to the higher selectivity to ethanol observed in Rh/MCM-41 (24%) compared to Rh/SiO$_2$ (8%).

Acknowledgments

Author Contributions

The experimental work and drafting of the manuscript was done by L.L., assisted by J.V., who carried out some catalyst characterization at KTH, and V.M., who performed the TEM measurements. M.B. and S.J. have supervised the experimental work and participated in the analysis and interpretation of the results. A.M., S.C., M.B. and S.J. supported the work and cooperation between KTH, UMSA and the University of Córdoba. The manuscript was written through the comments and contributions of all authors. All authors have approved for the final version of the manuscript.

Conflicts of Interest

The authors declare no conflicts of interest.

References

1. International Energy Agency. *Renewable Energy: Medium-Term Market (Market Trends and Projections to 2018)*; International Energy Agency—IEA: Paris, France, 2013.
2. Du, X.; Carriquiry, M.A. Flex-fuel vehicle adoption and dynamics of ethanol prices: Lessons from Brazil. *Energy Policy* **2013**, *59*, 507–512.
3. Licht, F.O. Ethanol Industry Outlook 2008–2013 Reports. Available online: http://www.afdc.energy.gov/data/ (accessed on 9 September 2014).
4. Chabrelie, M.F.; Gruson, J.F.; Sagnes, C. *Overview of Second-Generation Biofuel Projects*; IFP Energies Nouvelles: Paris, Fance, 2014.
5. Brown, R.C. *Thermochemical Processing of Biomass Conversion into Fuels, Chemicals and Power*; Wiley: Chichester, West Sussex, UK, 2011.
6. Suarez Paris, R.; Lopez, L.; Barrientos, J.; Pardo, F.; Boutonnet, M.; Jaras, S. Chapter 3 catalytic conversion of biomass-derived synthesis gas to fuels. In *Catalysis: Volume 27*; The Royal Society of Chemistry: London, UK, 2015; Volume 27, pp. 62–143.
7. Spivey, J.J.; Egbebi, A. Heterogeneous catalytic synthesis of ethanol from biomass-derived syngas. *Chem. Soc. Rev.* **2007**, *36*, 1514–1528.
8. Subramani, V.; Gangwal, S.K. A review of recent literature to search for an efficient catalytic process for the conversion of syngas to ethanol. *Energy Fuels* **2008**, *22*, 814–839.
9. Ma, H.T.; Yuan, Z.Y.; Wang, Y.; Bao, X.H. Temperature-programmed surface reaction study on C_2-oxygenate synthesis over sio$_2$ and nanoporous zeolitic material supported Rh-Mn catalysts. *Surf. Interface Anal.* **2001**, *32*, 224–227.

10. Chen, G.; Guo, C.Y.; Zhang, X.; Huang, Z.; Yuan, G. Direct conversion of syngas to ethanol over Rh/Mn-supported on modified SBA-15 molecular sieves: Effect of supports. *Fuel Process. Technol.* **2011**, *92*, 456–461.

11. Chen, G.; Guo, C.-Y.; Huang, Z.; Yuan, G. Synthesis of ethanol from syngas over iron-promoted Rh immobilized on modified SBA-15 molecular sieve: Effect of iron loading. *Chem. Eng. Res. Des.* **2011**, *89*, 249–253.

12. Fechete, I.; Wang, Y.; Védrine, J.C. The past, present and future of heterogeneous catalysis. *Catal. Today* **2012**, *189*, 2–27.

13. Martínez, A.; Prieto, G. The application of zeolites and periodic mesoporous silicas in the catalytic conversion of synthesis gas. *Top. Catal.* **2009**, *52*, 75–90.

14. Kresge, C.T.; Leonowicz, M.E.; Roth, W.J.; Vartuli, J.C.; Beck, J.S. Ordered mesoporous molecular sieves synthesized by a liquid-crystal template mechanism. *Nature* **1992**, *359*, 710–712.

15. Biz, S.; Occelli, M.L. Synthesis and characterization of mesostructured materials. *Catal. Rev.* **1998**, *40*, 329–407.

16. Arakawa, H.; Takeuchi, K.; Matsuzaki, T.; Sugi, Y. Effect of metal dispersion on the activity and selectivity of Rh/SiO$_2$ catalyst for high pressure co hydrogenation. *Chem. Lett.* **1984**, *13*, 1607–1610.

17. Underwood, R.P.; Bell, A.T. Influence of particle size on carbon monoxide hydrogenation over silica- and lanthana-supported rhodium. *Appl. Catal.* **1987**, *34*, 289–310.

18. Tago, T.; Hanaoka, T.; Dhupatemiya, P.; Hayashi, H.; Kishida, M.; Wakabayashi, K. Effects of Rh content on catalytic behavior in CO hydrogenation with Rh-silica catalysts prepared using microemulsion. *Catal. Lett.* **2000**, *64*, 27–31.

19. Zhou, S.T.; Zhao, H.; Ma, D.; Miao, S.J.; Cheng, M.J.; Bao, X.H. The effect of Rh particle size on the catalytic performance of porous silica supported rhodium catalysts for co hydrogenation. *Z. Phys. Chem.* **2005**, *219*, 949–961.

20. Lopez, L.; Velasco, J.; Cabrera, S.; Boutonnet, M.; Järås, S. Effect of syngas conversion and catalyst reduction temperature in the synthesis of ethanol: Concentration of water vapor in mesoporous Rh/MCM-41 catalyst. *Catal. Commun.* **2015**, *69*, 183–187.

21. Khodakov, A.Y.; Zholobenko, V.L.; Bechara, R.; Durand, D. Impact of aqueous impregnation on the long-range ordering and mesoporous structure of cobalt containing MCM-41 and SBA-15 materials. *Microporous Mesoporous Mater.* **2005**, *79*, 29–39.

22. Landau, M.V.; Varkey, S.P.; Herskowitz, M.; Regev, O.; Pevzner, S.; Sen, T.; Luz, Z. Wetting stability of Si-MCM-41 mesoporous material in neutral, acidic and basic aqueous solutions. *Microporous Mesoporous Mater.* **1999**, *33*, 149–163.

23. Borodziński, A.; Bonarowska, M. Relation between crystallite size and dispersion on supported metal catalysts. *Langmuir* **1997**, *13*, 5613–5620.

24. Ehwald, H.; Ewald, H.; Gutschick, D.; Hermann, M.; Miessner, H.; Ohlmann, G.; Schierhorn, E. A bicomponent catalyst for the selective formation of ethanol from synthesis gas. *Appl. Catal.* **1991**, *76*, 153–169.

25. Wong, C.; McCabe, R.W. Effects of oxidation/reduction treatments on the morphology of silica-supported rhodium catalysts. *J. Catal.* **1987**, *107*, 535–547.

26. Robertson, S.D.; McNicol, B.D.; de Baas, J.H.; Kloet, S.C.; Jenkins, J.W. Determination of reducibility and identification of alloying in copper-nickel-on-silica catalysts by temperature-programmed reduction. *J. Catal.* **1975**, *37*, 424–431.

27. Panpranot, J.; Goodwin, J.G., Jr.; Sayari, A. Synthesis and characteristics of MCM-41 supported coru catalysts. *Catal. Today* **2002**, *77*, 269–284.

28. Mei, D.; Rousseau, R.; Kathmann, S.M.; Glezakou, V.-A.; Engelhard, M.H.; Jiang, W.; Wang, C.; Gerber, M.A.; White, J.F.; Stevens, D.J. Ethanol synthesis from syngas over Rh-based/SiO$_2$ catalysts: A combined experimental and theoretical modeling study. *J. Catal.* **2010**, *271*, 325–342.

29. Chuang, S.C.; Stevens, R., Jr.; Khatri, R. Mechanism of C$_{2+}$ oxygenate synthesis on Rh catalysts. *Top. Catal.* **2005**, *32*, 225–232.

30. Hansen, J.B.; Højlund Nielsen, P.E. Methanol synthesis. In *Handbook of Heterogeneous Catalysis*; Ertl, G., Knözinger, H., Weitkamp, J., Eds.; VCH: Weinheim, Germany, 2008.

31. Bowker, M. On the mechanism of ethanol synthesis on rhodium. *Catal. Today* **1992**, *15*, 77–100.

32. Medford, A.J.; Lausche, A.C.; Abild-Pedersen, F.; Temel, B.; Schjodt, N.C.; Norskov, J.K.; Studt, F. Activity and selectivity trends in synthesis gas conversion to higher alcohols. *Top. Catal.* **2014**, *57*, 135–142.

33. Choi, Y.M.; Liu, P. Mechanism of ethanol synthesis from syngas on Rh(111). *J. Am. Chem. Soc.* **2009**, *131*, 13054–13061.

34. Cabrera, S.; El Haskouri, J.; Guillem, C.; Latorre, J.; Beltrán-Porter, A.; Beltrán-Porter, D.; Marcos, M.D.; Amorós, P. Generalised syntheses of ordered mesoporous oxides: The atrane route. *Solid State Sci.* **2000**, *2*, 405–420.

35. El Haskouri, J.; Cabrera, S.; Guillem, C.; Latorre, J.; Beltrán, A.; Beltrán, D.; Marcos, M.D.; Amorós, P. Atrane precursors in the one-pot surfactant-assisted synthesis of high zirconium content porous silicas. *Chem. Mater.* **2002**, *14*, 5015–5022.

36. Bartholomew, C.H.; Farrauto, R.J. *Fundamentals of Industrial Catalytic Processes*, 2nd ed.; Wiley-Interscience: Hoboken, NJ, USA, 2006.

37. Webb, P. *Introduction to Chemical Adsorption Analytical Techniques and Their Applications to Catalysis*; Micromeritics Instrument Corp.: Norcross, GA, USA, 2003.

38. Andersson, R.; Boutonnet, M.; Järås, S. On-line gas chromatographic analysis of higher alcohol synthesis products from syngas. *J. Chromatogr. A* **2012**, *1247*, 134–145.

39. Elsevier. Chapter 15 quantitative analysis by gas chromatography measurement of peak area and derivation of sample composition. In *Journal of Chromatography Library*; Georges, G., Claude, L.G., Eds.; Elsevier: Amsterdam, The Netherlands; Oxford, UK; New York, NY, USA; Tokyo, Japan, 1988; Volume 42, pp. 629–659.

40. Madon, R.J.; Boudart, M. Experimental criterion for the absence of artifacts in the measurement of rates of heterogeneous catalytic reactions. *Ind. Eng. Chem. Fund.* **1982**, *21*, 438–447.